Investigating demyelination, iron accumulation, and synaptic loss in Alzheimer's disease using multimodal imaging techniques

Soodeh Moallemian, Eric Salmon, Mohamed Ali Bahri, Nikita Beliy, Emma Delhaye, Evelyne Balteau, Christian Degueldre, Christophe Phillips* & Christine Bastin*

GIGA-Cyclotron Research Centre-in vivo imaging, University of Liège, Allée du 6 Août, B30, 4000 Liege, Belgium

* These authors contributed equally to this work

Correspondence: Christine Bastin and Christophe Phillips, GIGA-Cyclotron Research Centre-in vivo imaging, University of Liège, Allée du 6 Août, B30, 4000 Liège, Belgium, Phone: +32 4 366 23 16, Email: Christine.Bastin@uliege.be ; c.phillips@uliege.be

Abstract

Alzheimer's disease (AD), the most common type of dementia, is associated with neuronal death and synaptic loss [1], [2]. Pathological aggregation of amyloid-beta and tau protein are key elements of AD pathophysiology. Myelin loss and iron accumulation in the brain are also fundamental features of aging and dementia [3], [4], but are less frequently investigated. Quantitative MRI (qMRI) enables us to determine the brain tissue parameters such as magnetization transfer (MT) and effective transverse relaxation (R2*), which leads to the detection of microstructural tissue-related alterations in aging and neurodegenerative diseases [5].

Here we investigate the association of neurodegeneration (as indexed by loss of synaptic density), increased iron accumulation, and decreased myelination in Alzheimer's disease in cohorts of 24 amyloid-positive patients (AD, 11 males and 13 females) and 19 healthy controls (HC, 9 males, and 10 females). All participants underwent a multiparameter qMRI protocol, which was processed to generate probability maps for MTsat and R2* [5]. Synaptic density was evaluated by the total volume distribution (Vt)maps, representing the distribution of the [18F] UCB-H PET radiotracer in the brain [6].

The data is organized according to the Brain Imaging Data Structure (BIDS) [7]. MRI data processing was performed in MATLAB (The MathWorks Inc., Natick, MA, USA) using the SPM12 framework (www.fil.ion.ucl.ac.uk/spm) and the hMRI toolbox [8] after modifications to make MR data compatible with the BIDS format [9]. Each multi-parameter map presents a different tissue-related (semi-)quantitative property, and therefore the qMRI maps have specific units. Therefore, all maps were z-transformed to ensure the comparability of the maps in a multivariate model. Then, we used General Linear Model (GLM) to test the groups against each other using age and sex as the covariates. Also, a multivariate GLM (mGLM) was performed on all modalities using the MSPM toolbox (https://github.com/LREN-CHUV/MSPM) to test differences in groups controlling for the age and sex of the participants [10].

Univariate group analysis of MTsat data resulted in a significant difference at the cluster level in the right hippocampus with p_cluster<0.05 FWE corrected and p_voxel<.001 uncorrected as cluster forming threshold (Figure1.A). In contrast, the same analysis for R2* modality reveals no difference between the groups. PET_Vt maps showed a difference between AD and HC at p_voxel<0.05 (FWE corrected) in the right amygdala and hippocampus (Figure1.B), which agrees with previously reported results in [6]. See table.1 for more information.

Multimodal analysis combining R2*, MTsat, and PET_Vt shows a bilateral difference in hippocampus between patients and healthy controls for voxel-wise analysis with corrected FWE P-voxel < 0.05 (Figure1.C). The canonical analysis suggests that AD patients had combined decreased myelination, decreased synaptic density, and increased iron in the hippocampus compared to controls.

To conclude, in case of AD, there is an interaction between neuropathological risk factors, therefore, to restrain the true multivariate nature of the data and better control for the false positive rate, one should use the multivariate model over multiple univariate models.

Keywords: Alzheimer's disease, qMRI, PET, Multivariate analysis

References

[1] M. Calabrò, C. Rinaldi, G. Santoro, and C. Crisafulli, "The biological pathways of Alzheimer disease: a review," *AIMS Neurosci.*, vol. 8, no. 1, pp. 86–132, Dec. 2020, doi: 10.3934/Neuroscience.2021005.

[2] S. Azam, M. E. Haque, R. Balakrishnan, I.-S. Kim, and D.-K. Choi, "The Ageing Brain: Molecular and Cellular Basis of Neurodegeneration," *Front. Cell Dev. Biol.*, vol. 9, p. 683459, 2021, doi: 10.3389/fcell.2021.683459.

[3] G. Bartzokis, "Age-related myelin breakdown: a developmental model of cognitive decline and Alzheimer's disease," *Neurobiol. Aging*, vol. 25, no. 1, pp. 5–18, Jan. 2004, doi: 10.1016/j.neurobiolaging.2003.03.001.

[4] J. Acosta-Cabronero, M. J. Betts, A. Cardenas-Blanco, S. Yang, and P. J. Nestor, "*In Vivo* MRI Mapping of Brain Iron Deposition across the Adult Lifespan," *J. Neurosci.*, vol. 36, no. 2, pp. 364–374, Jan. 2016, doi: 10.1523/JNEUROSCI.1907-15.2016.

[5] N. Weiskopf *et al.*, "Quantitative multi-parameter mapping of R1, PD*, MT, and R2* at 3T: a multi-center validation," *Front. Neurosci.*, vol. 7, 2013, doi: 10.3389/fnins.2013.00095.

[6] C. Bastin *et al.*, "In vivo imaging of synaptic loss in Alzheimer's disease with [18F]UCB-H positron emission tomography," *Eur. J. Nucl. Med. Mol. Imaging*, vol. 47, no. 2, pp. 390–402, Feb. 2020, doi: 10.1007/s00259-019-04461-x.

[7] K. J. Gorgolewski *et al.*, "The brain imaging data structure, a format for organizing and describing outputs of neuroimaging experiments," *Sci. Data*, vol. 3, no. 1, p. 160044, Dec. 2016, doi: 10.1038/sdata.2016.44.

[8] K. Tabelow *et al.*, "hMRI – A toolbox for quantitative MRI in neuroscience and clinical research," *NeuroImage*, vol. 194, pp. 191–210, Jul. 2019, doi: 10.1016/j.neuroimage.2019.01.029.

[9] A. Karakuzu *et al.*, "qMRI-BIDS: An extension to the brain imaging data structure for quantitative magnetic resonance imaging data," *Sci. Data*, vol. 9, no. 1, Art. no. 1, Aug. 2022, doi: 10.1038/s41597-022-01571-4.

[10] L. Gyger *et al.*, "Temporal trajectory of brain tissue property changes induced by electroconvulsive therapy," *NeuroImage*, vol. 232, p. 117895, May 2021, doi: 10.1016/j.neuroimage.2021.117895.

Figures and tables:

Table 1. Statistical analysis of Mtsat, R2, and PET_vt maps for two groups of AD and HC. P-value*: P-value for FWE corrected at cluster level analysis. (df=39 for the univariate analysis and df=37 for the multivariate analysis)*

Cluster number	Coordinate at peak	F-Value at peak	Cluster P-value*	Cluster size	Brain region
Mtsat (P<0.001 FWE uncorrected at voxel level analysis)					
1	(28 –7 –27)	26.58	0.002	1993	Right hippocampus
PET_vt (P<0.05 FWE corrected at voxel level analysis)					
1	(25,-10,-14)	64.16		8	Right hippocampus
2	(14,-10,-21)	64.07		2	Right hippocampus
3	(18,-11,-13)	63.74		5	Right amygdala
Multimodal (P<0.05 FWE corrected at voxel level analysis)					
1	(25,-10,-14)	21.11		8	Right hippocampus
2	(-27,-12,-15)	50.10		11	Left hippocampus
3	(35,-18,-13)	34.02		5	Right hippocampus

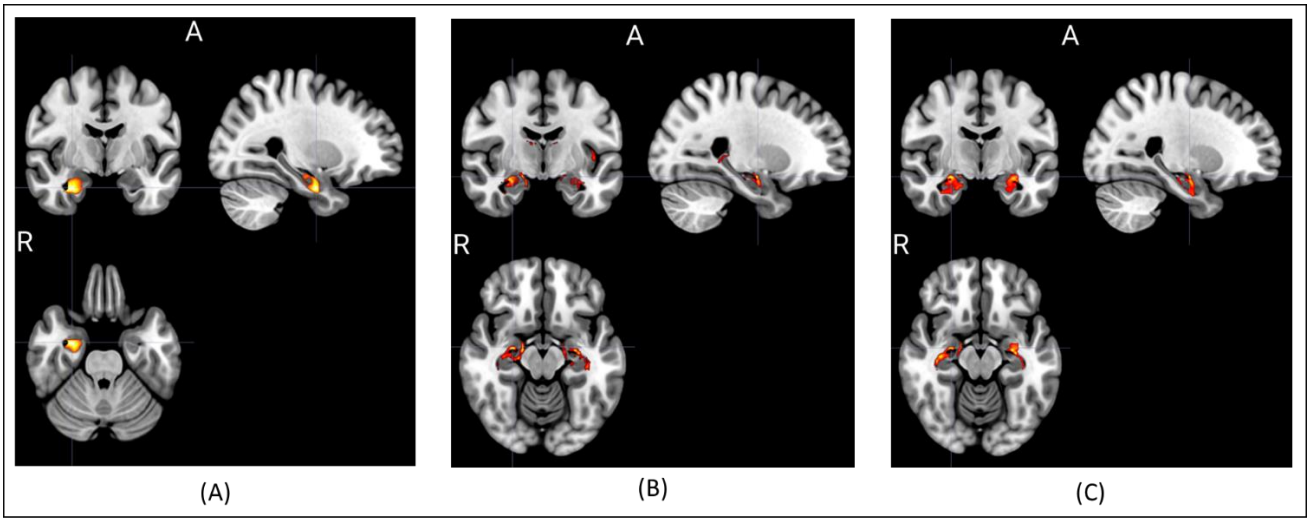

Figure 1. Statistical parametric map of A) Mtsat maps, B) PET_vt maps, and C) Multimodal association with changes in microstructural changes and synaptic density between AD and HC groups. For presentation purposes displayed at p < .001 voxel-wise uncorrected

Synopsis:

We used qMRI and [18F]UCBH-PET data to investigate the co-occurrence of demyelination, iron accumulation, and loss of synaptic density in the brain which are AD risk factors. Univariate GLM analysis shows a significant difference between two groups of AD patients and healthy controls in the hippocampus for Mtsat (proportional to myelin) and PET_Vt maps (representing synaptic density). Multivariate GLM resulted in a significant difference at the voxel level ($p<0.05$) in the hippocampus. Canonical analysis reveals that an increase in the iron level is associated with demyelination and synaptic loss bilaterally in the hippocampus.